Romanian Reports in Physics **69**, 404 (2017)

A METHOD OF VIRTUAL IMAGE FOR DETERMINATION OF NEGATIVE REFRACTION INDEX OF A NANOMEDIUM

V. SERGENTU[1], V. URSAKI[2]

[1]Institute of Applied Physics of the Academy of Sciences of Moldova, 5 Academy Street, MD-2028 Chisinau, Moldova, E-mail: vsergentu@yahoo.com
[2]Institute of Electronic Engineering and Nanotechnology of the Academy of Sciences of Moldova, Academy str. 3/3, MD-2028 Chisinau, Moldova, E-mail: ursaki@yahoo.com

Received May 15, 2016

Abstract. In this paper we propose a method for measuring the negative refraction index of films of optically transparent materials. The method is based on recording the direction of propagation and the shifting of the ray reflected from the film. It is shown that the method can be applied for both macroscopic and nanometric samples. However, a precise control of parameters of the radiation source is needed for using this method in the case of nanometric samples. The conditions for a composite medium to acquire a negative refractive index are discussed.

Key words: optical nanomedium, metamaterial, negative refraction index, wave front, quasi-plane wave, optical impedance.

1. INTRODUCTION

New nanomedia with unusual properties are nowadays in the focus of attention of many research groups. Optical nanomedia with negative refraction index are of especial interest [1, 2, 3]. However, all the used metamaterials represent systems of heterogeneous elements with substantially different properties, and there is a contradiction when dealing with such systems. On the one hand, one has to use components with dramatically different properties. On the other hand, one has to get a substantially homogeneous optical metamaterial for wavelengths of radiation comparable with the mean distance between the elements. Actually, a heterogeneous system consisting of individual particles can behave like a virtually homogeneous optical metamaterial independently on the wavelength of radiation, if some specific conditions are satisfied. However, one needs to have a simple and reliable method for the determination of optical parameters of metamaterials in order to be able to control the fulfillment of these conditions. The usual scheme for measuring the negative refraction index of a plate of a transparent material implies measuring the parameters of the real image of a point source of radiation. However, the experimental methods for testing such properties require

sophisticated tools of nanomeasurements [4, 5]. Apart from this, such a scheme is actually applicable only for the case of $n = 1$, when $\varepsilon = \mu = -1$ [6].

In this paper we propose to use a method based on the well known experimental technique for the investigation of Goos-Hänchen effect, which allows one to evaluate the degree of homogeneity and refraction coefficient of the medium [7].

2. A SIMPLE MODEL OF OPTICAL NANOMEDIUM WITH NEGATIVE REFRACTION INDEX

As mentioned above, usually the negative refraction index of a plate of a transparent material is measured on the basis of a scheme with the real image of a point source of radiation (Fig. 1).

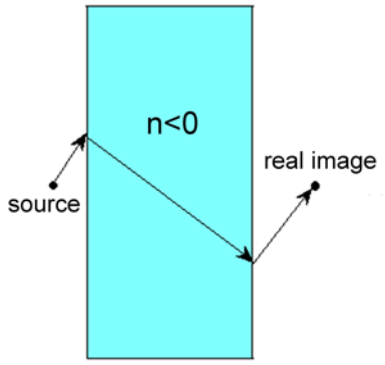

Fig. 1 – A usual scheme for the determination of the negative refraction index (the method of real image).

In contrast to this, we will use a method with a virtual image for the determination of negative refraction index of a nanomedium. The proposed method is suitable for various metamaterials [8, 9], including those with a subsystem of cylinders with negative refraction index [10]. Let us first consider a simple model of nanomaterial in the form of a system of nanocylinders immersed in vacuum. The nanocylinders with the axis oriented along the Z axis are arranged in a periodic two-dimensional array in the two-dimensional space $\vec{\rho} = [X, Y]$ with the lattice constant equal to a. The relative dielectric permittivity and magnetic permeability of such a system are changing in the space according to a periodic law $\mu \equiv \varepsilon = \varepsilon(\vec{\rho})$. In the vacuum $\varepsilon \equiv \mu = 1$, while inside cylinders $\mu \equiv \varepsilon = -1$. Let us assume that in a very thin boundary layer with thickness $\delta \to 0$ between the cylinder and the vacuum we have $\varepsilon(\vec{\rho}) \to 0$. The polarization vector of the incident radiation is directed along the cylinder axis.

We assume that the dispersion law is the main characteristic of the transparent optical medium. By using the standard method for the determination of the dispersion law for two-dimensional photonic crystals [11] we obtain

$$-\varepsilon(\vec{\rho})^{-1}\nabla(\varepsilon(\vec{\rho})^{-1}\nabla E(\vec{\rho})) = (\omega/c)^2 E(\vec{\rho}), \quad (1)$$

where $E(\vec{r})$ is the electric field strength, and ω is the frequency of the wave.

The equation (1) can be transformed into

$$\omega^{-2}\left[\nabla^2 E(\vec{\rho}) + \frac{1}{2}(\nabla \ln(\varepsilon^2(\vec{\rho})))\nabla E(\vec{\rho})\right] = -\varepsilon(\vec{\rho})^2 E(\vec{\rho}). \quad (2)$$

Since in the standard method of plane waves the matrix elements of the second term in the left-hand side of the equation (2) tend to zero $\delta \to 0$, one can keep only the first term in the left-hand side, and obtain

$$(\omega/c)^{-2}\nabla^2 E(\vec{\rho}) = -|\varepsilon(\vec{\rho})| E(\vec{\rho}). \quad (3)$$

The equation (3) for determination of eigenvalues of ω^{-2} is actually equivalent to a similar equation from ref. [11]. We see that the mathematical problem of finding the spectrum of electromagnetic oscillations for our system practically does not differ from a similar problem for a system of dielectric cylinders, but with substitution of $\varepsilon(\vec{r})$ by $|\varepsilon(\vec{r})| \equiv 1$. The spectrum of such a system does not differ from the spectrum of vacuum with the refraction index $n_{\text{eff}} = n_{\text{v}} = \pm 1$ (which is equivalent to $\mu_{\text{eff}} \equiv 1/\varepsilon_{\text{eff}}$). However, the system impedance $Z_{\text{eff}} = \mu_{\text{eff}}/\varepsilon_{\text{eff}}$ is different from the case of vacuum $Z_{\text{v}} \equiv 1$.

It is known [12, 13] that a usual composite medium behaves like a homogeneous medium with a definite refraction index, but only for $\lambda = 2\pi/k_0 >> a$. However, the considered in this paper system will behave like a homogeneous medium with a definite refraction index up to values of $\lambda \sim a$. The reason for this phenomenon was specified in ref. [14]. Each of transparent cylinders scatters the plane wave, mainly in the direction parallel to the direction of incident wave propagation [14] (Fig. 2). It can be argued that the inclusions from a conventional optically transparent material behave like scatterers. However, the inclusions from a metamaterial behave like scatterer antipodes.

The value of ε_{eff} for $\lambda > a$ can be estimated from the formula $\varepsilon_{eff} \cong (1-2c)$ [13], where c is the share of material in the volume of the metamaterial. One can see from this formula that $\mu_{eff}, \varepsilon_{eff} \approx -1$, $Z_{\text{eff}} \approx 1$ for $c \approx 1$ (large radii of the cylinders $R \approx a/2$). A simple case of vacuum ($\varepsilon_{eff} \equiv \mu_{eff} = 1$,

$Z_{\text{eff}} = 1$) is obtained with decreasing the radius of cylinders ($R \to 0$), while a case with $\varepsilon_{eff} \to 0$, $\mu_{eff} = 1/\varepsilon_{eff} \to \infty$, $|Z_{\text{eff}}| \to \infty$ is obtained for $c \to 1/2$.

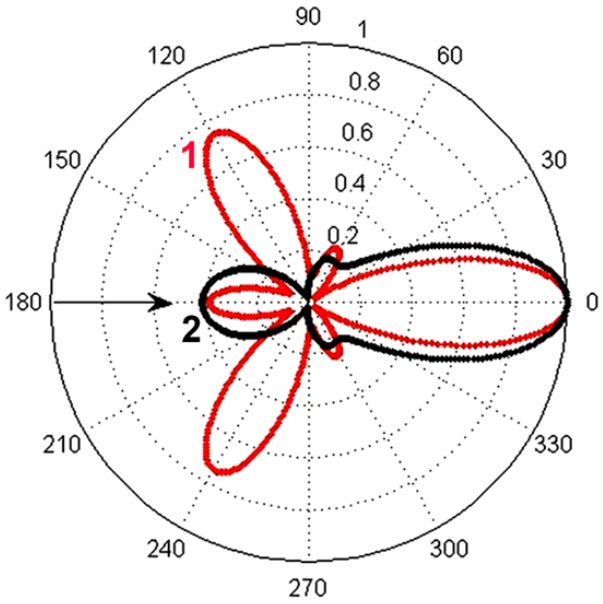

Fig. 2 – The scattering indicatrix of various types of transparent cylinders for the wavelength of $\lambda = 4R$. 1 is for a usual transparent material with $\varepsilon = 10$, and 2 is for a metamaterial with $\varepsilon = \mu = -1$.

Similar results with minor differences are obtained for the case when the polarization vector of the incident radiation is perpendicular to the cylinders axis. The larger is the radiation wavelength as compared to the lattice constant, the more applicable are the above mentioned conclusions.

3. DESCRIPTION OF THE METHOD ON THE EXAMPLE OF A SIMPLE MODEL OF OPTICAL NANOMEDIUM

The method is based on determination of parameters of the virtual image occurring at the incidence of a light beam on a plate of optically transparent material with parallel surfaces and refraction index n. The reflected ray shifts to different directions depending on the sign of the refraction index (Fig. 3). The observed virtual image of the light source also shifts in different directions relative to the mirror image at the interface medium/vacuum.

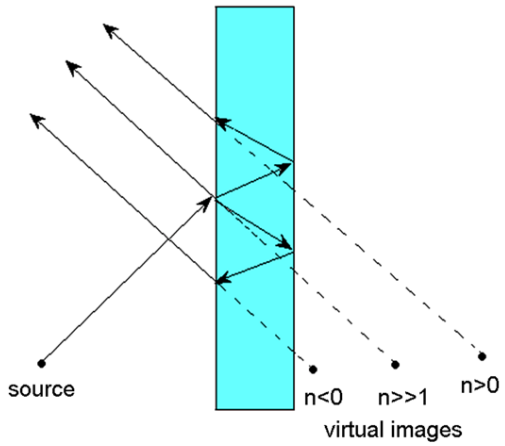

Fig. 3 – The reflected ray shifts to different directions depending on the sign of the refraction index. The observed virtual image of the light source also shifts in different directions. The ray shift is actually an analog of the Goos-Hänchen shift, but for our case.

We will assume in our further calculations that the plate with parallel surfaces is located at an ideally reflecting surface (Fig. 4). Practically any substrate with permittivity $\varepsilon >> 1$ satisfies this condition, since we will further deal with strongly etched samples with a share of material in the volume of the metamaterial of the order of several percents [15].

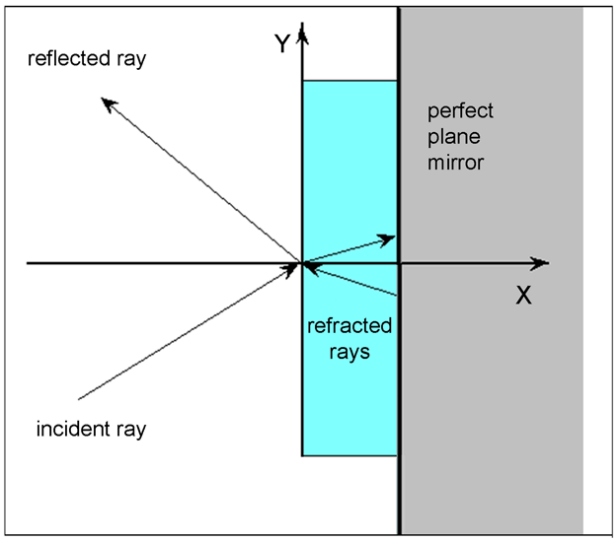

Fig. 4 – The phenomenon of refraction/reflection of the incident radiation for the case of a plate with parallel surfaces with ε_{eff}, μ_{eff} located at an ideally reflecting surface.

In the case of the electric field perpendicular to the plane of incidence of the ray we obtain [12]

$$E_1 = E_0 \exp(iS), \tag{4}$$

where E_1, E_0 are the amplitudes of the reflected and incident waves, d is the thickness of the plate.

$$S = -2\mathrm{arctg}\left(\frac{k_{2x}}{\mu_{eff} k_{0x}} \mathrm{ctg}(k_{2x} d) \right), \tag{5}$$

where $k_{0x} = \sqrt{k_0^2 - k_y^2}$, $k_{2x} = \sqrt{\varepsilon_{eff}\, \mu_{eff}\, k_0^2 - k_y^2}$.

The formula for the shift of the ray after passing through the plate is

$$\delta = (\partial S / \partial k_y), \tag{6}$$

For the case of $\varepsilon_{eff} = \mu_{eff} = \pm 1$ we have

$$\delta = \frac{2 k_y d}{\mu_{eff} \sqrt{k_0^2 - k_y^2}}, \tag{7}$$

from which it follows that $|\delta| \to \infty$ when $k_y \to k_0$, *i.e.* for large angles of incidence.

Further we will discuss the procedures for testing nanoplates. We will use a directional radiation source with an aperture ensuring obtaining a limited area of the planar wavefront near the sample surface, which will preserve this property at a distance L greater than the thickness of the layer d. Let us name it quasi-plane wavefront. We will further use in our calculations a light source radiating in the direction of the angle $\theta_0 = \pi / 4$. The wave field is described by the formula

$$E(\rho, \theta) = \sum_{l=-M}^{M} \exp(il(\theta - \theta_0 + \pi/2)) H_l^{(1)}(k\rho), \tag{8}$$

where $H_l^{(1)}$ is the Hankel function. A wave beam with

$E(\rho, \theta)\big|_{\rho \to \infty} \to 2\sqrt{2\pi / \rho} \exp(-i\pi/4) \delta(\theta - \theta_0)$ is obtained at $M \to \infty$.

This type of two-dimensional diffractionless wave field (self-reconstructing light beam) is analogous to Bessel beams [16]. The radiation aperture is $\Delta\theta \approx 1/M$ in the case of a finite $M >> 1$. If the condition $M \approx kR/\pi$ (R is the distance from the emitter to the center of the plate) is satisfied for a wave-region of the radiation,

then the width of the beam in this region satisfies the condition of $R\Delta\theta > \lambda$ and, at the same time, $R >> \lambda$. The length of the used region of the beam L is smaller than R, but it should satisfy the condition of L >> d. The parameters are chosen so that $M=10^2 >> 1$, $d > \lambda$ and the source is moved to a distance of $R = 50\lambda >> d, \lambda$.

A coefficient is introduced to assess the degree of perfection of the wave

$$K(r) = \left[\vec{H}(r)\vec{H}_0^*(r) + \vec{H}^*(r)\vec{H}_0(r)\right] \cdot \left[2\vec{H}_0(r)\vec{H}_0^*(r)\right]^{-1}, \quad (9)$$

where $\vec{H}_0, \vec{H}$ are the intensities of magnetic fields of the plane right-hand wave and the quasi-plane wave, respectively, for which the wave vectors and the electric field intensities coincide; r is the distance from the center of the beam to the source.

The value of K is an indicative of the difference of the quasi-plane wave from the ideally planar right-hand wave in the vacuum. If $K = 1$ and the intensity I in the center of the beam remains constant at the distance L, then these waves can be considered as practically indistinguishable at this distance (Fig. 5). Otherwise, there is a significant part of radiation in the wave which behaves like a left-hand wave when it is incident at the plane surface boundary. The radiation is diffracted to an opposite diffraction angle as compared to the expected one, which can completely distort the measurement results by using a quasi-plane wave.

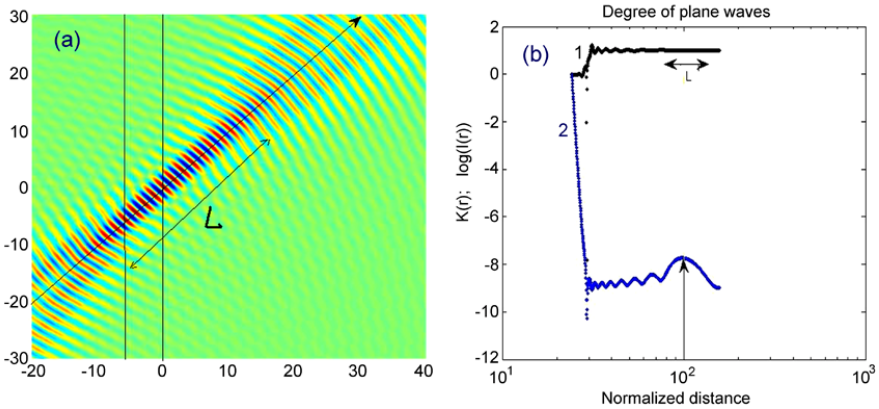

Fig. 5 – (a) Wave field of the radiation source near the sample surface ($M = 100$). The radiation beam ensures obtaining a quasi-plane wave front with a limited area. The beam length L is finite, but it is larger that the plate thickness and the wavelength; b) the dependence of the coefficient K (curve 1) and the intensity $\log(I)$ in the center of the beam (curve 2) on the normalized distance ($2r/\lambda$) from the source. The arrow indicates the region where the radiation beam can be considered to be quasi-plane.

Let us first consider a simple model of the matter as a perfectly homogeneous material with known parameters, and construct the wave field Real($E(\rho)$) near the nanosamples with an incident quasi-plane wave (Fig. 6). The formula (4) and the Matlab fft and ifft operators are used. The incident wave is not

taken into consideration when the image of the wave field is constructed, since it will disturb the observation of main regularities of the investigated phenomenon. At the same time, the arrows on drawings indicate the trajectories of two rays (the incident ray and the ray reflected from the center of the rear surface of the nanoplate).

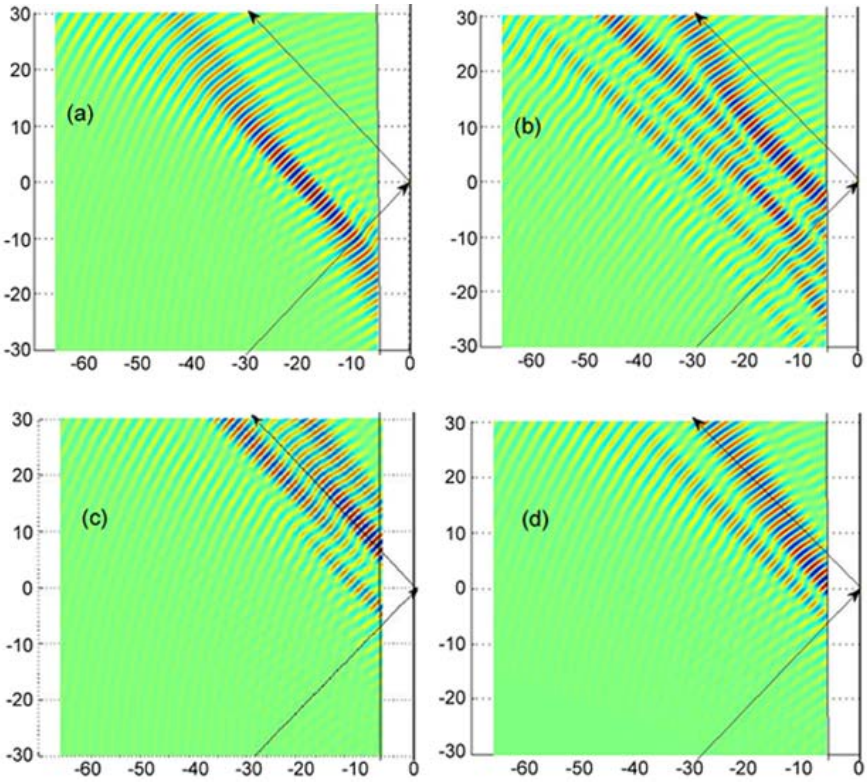

Fig. 6 – The wave field Real($E(\rho)$) near the nanosamples with an incident quasi-plane wave with wavelength $\lambda = 0.4$d for: (a) a metamaterial with $n_{eff} = -1$, $Z_{eff} = 1$; (b) a metamaterial with $n_{eff} = -1$, $Z_{eff} = 40$; (c) a metamaterial with $n_{eff} = 1$, $Z_{eff} = 6$; (d) a usual transparent material with $n = 3$, $Z = 0.11$.

The drawings in Fig. 6 are easily and simply interpreted. Fig. 6a illustrates the shift of a single beam for a medium with the refraction index $n_{eff} = -1$. There are no reflections from the material surface, and the optical impedance of the nanomaterial is $Z_{eff} = 1$. The beam is shifted to the left. Fig. 6b illustrates the shift of the beam for a medium with the refraction index $n_{eff} = -1$ and the optical impedance of the nanomaterial $|Z_{eff}| >> 1$. The first beam is the ray reflected from the surface of the nanomaterial, since $Z_{eff} \neq 1$. Other rays manifest theirselfs after reflections from the perfectly reflecting surface, and/or from the surface of the

nanomaterial. The shift of the beam for a medium with the refraction index $n = 1$ and the optical impedance of the nanomaterial $|Z_{\text{eff}}| >> 1$ is shown in Fig. 6c. The first weak beam is the ray reflected from the surface of the nanomaterial, since $Z_{\text{eff}} \neq 1$. Another ray (shifted to the right) emerges after reflection from the perfectly reflecting surface. Figure 6d shows the shift of the beam for a medium with the refraction index $n = 3.5$ and the optical impedance $Z = 0.11$. The first weak beam is the ray reflected from the surface of the nanomaterial. Another ray emerges after reflection from the perfectly reflecting surface.

Therefore, one can argue that the radiation source and the proposed method are consistent with the considered problem.

Similar results with minor differences are obtained for the case when the polarization vector of the incident radiation is perpendicular to the cylinders axis. The larger is the radiation wavelength as compared to the lattice constant, the more applicable are the above mentioned conclusions.

4. A NANOMEDIUM IN A REALISTIC MODEL

Further we consider a case of nanosample testing in the frame of a more complex and realistic model for the matter of the plate. All the used metamaterials represent systems from individual elements with different properties. The proposed method allows a detailed taking into consideration of the phenomenon of radiation scattering on individual elements of the medium. The metamaterial is modeled as a plate consisting of a system of different nanocylinders with known refraction indexes immersed in the vacuum. The cylinders are arranged in a trigonal lattice. A multiple scattering approach is used for calculations [17]. Near the j^{th} cylinder the electromagnetic field can be represented as

$$E(\vec{\rho}) = \sum_{m=-l}^{l} \left[\alpha_m(j) J_m(k_0\rho) + B_m(j) H_m^{(1)}(k_0\rho_{\rho j})\right] \exp(i\theta_{\rho j} m), \qquad (10)$$

where $\vec{\rho}_{\rho j} = \vec{\rho}_{\rho} - \vec{\rho}_j = (\rho_{\rho j}, \theta_{\rho j})$.

The relationship between the $\alpha_m(j)$ and $B_m(j)$ coefficients is given by

$$D_m(j) = B_m(j) / \alpha_m(j), \qquad (11)$$

where $D_m(j)$ appears from solving the problem of a single cylinder.

There is a system of equations for the self-consistent solution for all the cylinders

$$\widetilde{B}_m(i) = \alpha_m D_m(i) + \sum_{j \neq i} \sum_{l=-\infty}^{+\infty} \widetilde{B}_l(j) D_m(i) \exp(i(l-m)(\theta_{ij} + \pi)) H_{l-m}^{(1)}(k_0\rho_{ij}), \qquad (12)$$

where $\vec{\rho}_{ij} = \vec{\rho}_j - \vec{\rho}_i = (\rho_{ij}, \theta_{ij})$.

A problem of calculating the distribution of wave fields in the space around the system of cylinders arises after solving the equations. A simple technique is used. A cylinder with an extremely small radius, which practically does not scatter the incident radiation, is inserted at the point in space where the field amplitude has to be found. Then, the field amplitude is determined from the perturbation theory, and it is proportional to

$$\widetilde{W}_0(i) = \sum_{j \neq i} \sum_{l=0}^{\infty} \widetilde{B}_l(j) \exp(-il(\theta_{ji} + \pi)) H_l^{(1)}(k_0 \rho_{ji}) . \tag{13}$$

The nanoplate is placed on an infinitely conductive substrate, which serves at the same time as a symmetry plane for all the system. Therefore, instead of the system (13) we have

$$\begin{aligned} \widetilde{B}_m^{(+)}(i) = \alpha_m^{(+)} D_m(i) - D_m(i) \sum_{l=-\infty}^{\infty} \widetilde{B}_l^{(+)}(i) \exp(-i(l+m)(\theta_{ii}^{(+,-)} + \pi)) H_{-l-m}^{(1)}(k_0 \rho_{ii}^{(+,-)}) + \\ + \sum_{j \neq i} D_m(i) \sum_{l=-\infty}^{+\infty} \widetilde{B}_l^{(+)}(j) \begin{bmatrix} \exp(i(l-m)(\theta_{ij}^{(+,+)} + \pi)) H_{l-m}^{(1)}(k_0 \rho_{ij}^{(+,+)}) - \\ - \exp(-i(l+m)(\theta_{ij}^{(+,-)} + \pi)) H_{-l-m}^{(1)}(k_0 \rho_{ij}^{(+,-)}) \end{bmatrix} \end{aligned} \tag{14}$$

where $\vec{\rho}^{(+)} \equiv \vec{\rho}$, $\vec{\rho}^{(-)} = -\vec{i}_x x + \vec{i}_y y$, and, for instance,

$$\vec{\rho}_{ij}^{(+-)} = \vec{\rho}_j^{(-)} - \vec{\rho}_i^{(+)} = (\rho_{ij}^{(+-)}, \theta_{ij}^{(+-)}) .$$

These formulas allows one to construct the wave field Real($E(\rho)$) near the nanosamples upon the incidence of a quasi-plane wave.

Figure 7 is simply interpreted when compared with the simple model applied in Fig. 6. The similarity with the simple model is more pronounced with increasing the radiation wavelength. Figure 7a is similar to Fig. 6a, but with a more realistic model of the finite size of the system. The larger is the wavelength, the better is the similarity. Figure 7b is similar to Fig. 6b. The first beam is the ray reflected from the nanomaterial surface (the optical impedance of the nanomaterial $|Z| >> 1$). Another ray emerges after reflection from the ideally reflecting surface. A shift to the left is observed, similarly to a medium with refraction index $n = -1$. In Fig. 7c, which corresponds to cylinders from a material with refraction index $n = 3.2$ ($\varepsilon = 10$) and the impedance $Z = 0.1$, a ray reflected exactly from the place of entrance into the nanomaterial is observed. In contrast to Fig. 6d, the refracted ray is absent, since the medium is not homogeneous. The coherent beam in the medium is attenuated, and is quickly scattered in all the directions. Fig. 7d corresponds to a medium composed of two types of cylinders: 75% of them have the refraction index $n = 3.2$ (the optical impedance of the nanomaterial is $|Z| < 1$), and 25% of

them have the refraction index $n = -1$ (the optical impedance of the nanomaterial is $Z_{\text{eff}} = 1$). A partial homogenization of the material occurs in this case. The reflected ray is shifted from the place of entrance into the plate. It means that it was refracted, it entered into the material, and it was reflected from the mirror-like surface. At the same time, it was partially scattered.

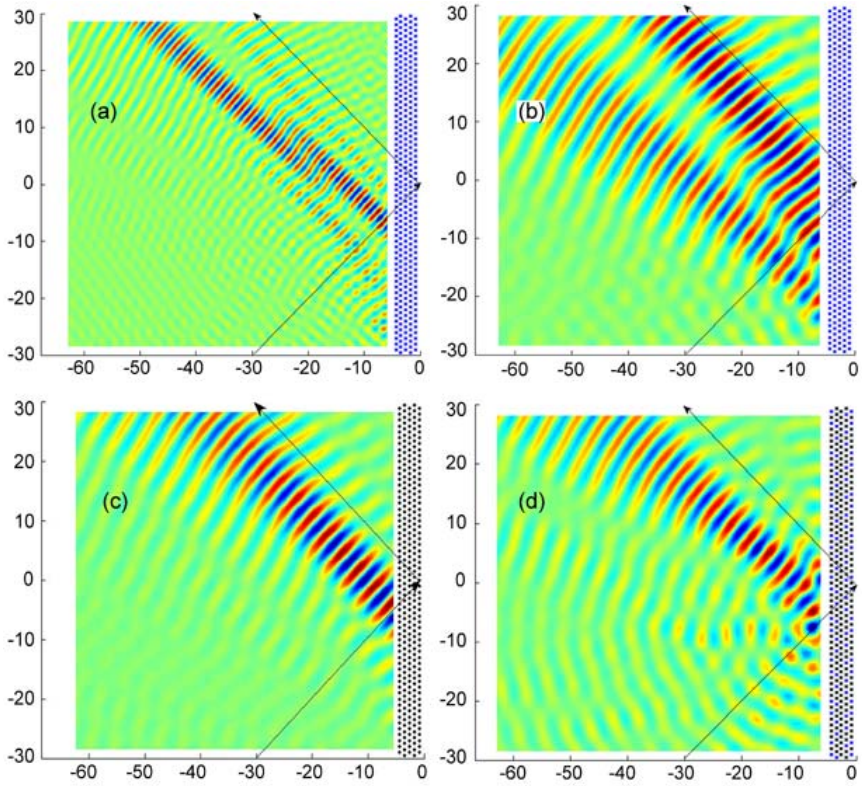

Fig. 7 – The wave field Real($E(\rho)$) near the nanosamples with an incident quasi-plane wave for: (a) cylinders from a metamaterial with $\mu_{\text{eff}} = \varepsilon_{\text{eff}} = -1$, the radius $R = 0.5a$, the wavelength $\lambda = 2a$; (b) cylinders from a metamaterial with $\mu_{\text{eff}} = \varepsilon_{\text{eff}} = -1$, the radius $R = 0.4a$, the wavelength $\lambda = 4a$; (c) cylinders from a usual transparent material with $\varepsilon = 10$, the radius $R = 0.5a$, the wavelength $\lambda = 4a$; (d) cylinders with radius $R = 0.5a$ are from two types of materials: 25% are from a metamaterial with $\mu_{\text{eff}} = \varepsilon_{\text{eff}} = -1$ and 75% are from a usual transparent material with $\varepsilon = 10$, the wavelength $\lambda = 4a$.

Similarly to Fig. 7, Fig. 8 illustrates the wave field for a medium composed of two types of cylinders, but with an inverse proportion of the constituents. One type of cylinders (25% of them) are from a material with refraction index $n = 3.2$ (the optical impedance of the nanomaterial is $Z = 0.1$). Another type of cylinders (75% of them) are from a metamaterial with refraction index $n_{\text{eff}} = -1$ (the optical impedance of the nanomaterial is $Z = 1$). A partial dehomogenization of the

metamaterial occurs in this case, *i.e.* it starts to scatter that part of radiation which shifted the ray to the left in Fig. 7b.The ray refracted on the surface of nanoplate is scattered inside the medium. The phenomenon of refraction in a left-hand medium occurs *via* "trapping" [18], which is sensitive to scattering. This prevents the manifestation of the phenomenon of ray shifting (Fig. 7b). The scattering is weakned in Fig. 8b, which leads to the appearance of several weak scattered rays.

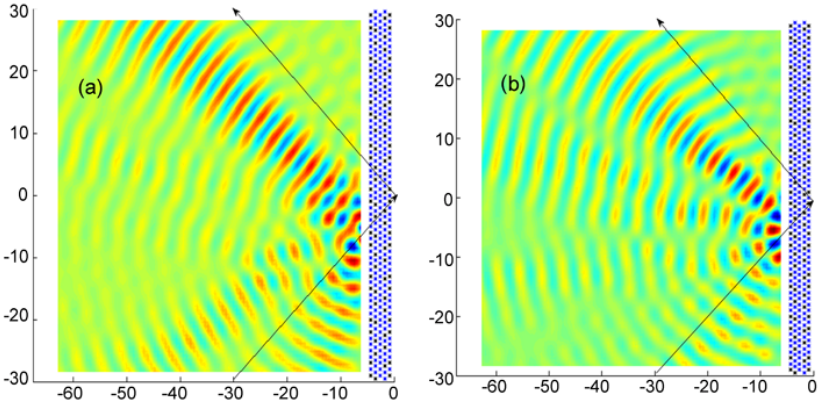

Fig. 8 – The wave field Real($E(\rho)$) near the nanosamples with an incident quasi-plane wave with wavelength $\lambda = 4a$ for a medium composed of two types of cylinders: one type of cylinders with radius R_1 (25% of them) are from a transparent material with $\varepsilon = 10$, while another type of cylinders with radius R_2 (75% of them) are from a metamaterial with $\mu_{\text{eff}} = \varepsilon_{\text{eff}} = -1$. The radii of cylinders are as follows: a) $R_1 = R_2 = 0.4a$; b) $R_1 = 0.25a$, $R_2 = 0.5a$.

If the scattering is reduced almost to zero as in the case illustrated in Fig. 9, then one of the weak scattered rays resembles the shifted ray from Fig. 7b.

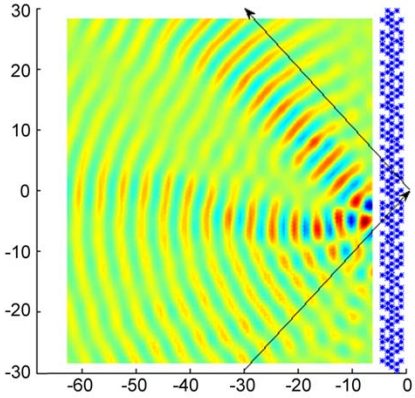

Fig. 9 – The wave field Real($E(\rho)$) near the nanosamples with an incident quasi-plane wave with wavelength $\lambda = 4a$ for a medium with 25% of empty space and 75% filled with cylinders of radius $R = 0.5a$ from a metamaterial with $\mu_{\text{eff}} = \varepsilon_{\text{eff}} = -1$.

5. CONCLUSIONS

A method is proposed for determination of parameters of media with negative refraction index. The method can be applied for both macroscopic and nanometric samples. A precise control of parameters of the radiation source is needed for using this method in the case of nanometric samples. One can judge about the optical parameters of the nanomedium by investigating the behavior of the reflected ray (the direction of propagation and the shifting of the reflected ray). When designing a metamaterial medium with negative refraction index, one needs to combine a scattering matrix from a material with usual refraction index with inclusion of a material with negative refraction index. With increasing the concentration of the inclusions, the scattering medium is gradually homogenized, it having a positive refraction index. However, the scattering is reduced to zero with a further increase of the inclusions concentration, and the medium acquires a negative refractive index.

Acknowledgments. This work was supported by the Academy of Sciences of Moldova under Grants Nos. 15.817.02.04A and 15.817.02.08A.

REFERENCES

1. W.J. Padilla, D.N. Basov, D.R. Smith, Materials Today **9**, 28-35 (2006).
2. S. Harvey, *Negative-Index Metamaterials*, University of Washington Pr., 2014.
3. I.M. Tiginyanu, E. Foca, V.V. Sergentu, V.V. Ursaki, F. Daschner, R. Knochel, and H. Foell, J. Nanoelectron. Optoe. **4**, 20-39 (2009).
4. N. Fang, H. Lee, C. Sun, X. Zhang, Science **308**, 534-537 (2005).
5. B. Bhushan (Ed.), *Springer Handbook of Nanotechnology*, Springer, Berlin, Heidelberg, 2010.
6. K. Yu. Bliokh, Yu. P. Bliokh, Phys. Usp. **47**, 393–400 (2004).
7. P.R. Bergman, Phys. Rev. E **66**, 067603 (2002);
   X. Yin, L. Hesselink, Z. Liu, N. Fang, X. Zhang, Appl. Phy. Lett. **85**, 372-375 (2004).
8. J. Li, L. Zhou, C.T. Chan, P. Sheng, Phys. Rev. Lett. **90**, 083901 (2003).
9. A.A. Asatryan, K.B. Dossou, L.C. Botten, *Local Density of States of Metamaterial Photonic Crystals, Australian Institute of Physics*, Proc. 18th National Congress, Adelaide, Australia, 2008.
10. V.V. Sergentu, V.V. Ursaki, I.M. Tiginyanu, F. Foca, H. Föll, Robert W. Boyd, Appl. Phys. Lett. **91**, 081103 (2007).
11. J.D. Joannopoulos, R.D. Meade, J.N. Winn, *Photonic Crystals: Modeling the Flow of Light*, Princeton Univ. Press, Princeton, NJ, 1995.
12. L.D. Landau, E.M. Lifshitz, L.P. Pitaevskii, *Electrodynamics of Continuous Media*, Butterworth-Heinemann, Oxford, 1984.
13. R. Landauer, AIP Conference Proceedings **40**, 2–45, American Institute of Physics, 1978.
14. A.E. Miroshnichenko, arXiv:0904.0153 [physics.optics] (2009).
15. S. Ya. Prislopski, E.K. Naumenko, I.M. Tiginyanu, L. Ghimpu, E. Monaico, L. Sirbu, S. V. Gaponenko. Optics Lett. **36**, 3227-3229 (2011).
16. D. Mcgloin, K. Dholakia, Contemp. Phys. **46**, 15-28 (2005).
17. X. Zhang, L.-M. Li, Z.-Q. Zhang, C. T. Chan, Phys. Rev. B **63**, 125114 (2001).
18. S. Foteinopoulou, E. N. Economou, C. M. Soukoulis, Phys. Rev. Lett. **90**, 107402 (2003).